Optimization of the Depth of Penetration by Welding Input Parameters in SAW Process Using Response Surface Methodology

MOHSEN KAZEMI, MASOOD AGHAKHANI, EHSAN HAGHSHENAS-JAZI, and ALI BEHMANESHFAR

The aim of this paper is to optimize the depth of penetration with regard to the effect of MgO nanoparticles and welding input parameters. For this purpose, response surface methodology (RSM) with central composite rotatable design (CCRD) was used. The welding current, arc voltage, nozzle-to-plate distance, welding speed, and thickness of MgO nanoparticles were determined as the factors, and depth of penetration was considered as the response. Quadratic polynomial model was used for determining the relationship between the response and factors. A reduced model was obtained from the data which the values of R^2, R^2 (pred), and R^2 (adj) of this model were 92.05, 69.05, and 86.31 pct, respectively. Thus, this model was suitable, and it was used to determine the optimum levels of factors. The results show that the welding current, arc voltage, and nozzle-to-plate distance factors should be adjusted in high level, and welding speed and thickness of MgO nanoparticles factors should be adjusted in low level.

DOI: 10.1007/s11663-015-0492-x

I. INTRODUCTION

In recent years, the research field of nanotechnology has attracted considerable attention of scientists and engineers. Nanostructure materials often are characterized by a grain size or the particulate size of up to about 100 nm. These materials are suitable candidates for different applications including aerospace, electronics, and automotive and chemical industries because of the reduction of the grain size in the nanometer scale and large surface area of nanoparticles offer unique mechanical, elevated temperature, electrical, magnetic, and optical properties.[1,2]

Among the new technologies in the field of materials joining together, the issue is related to nanotechnology and welding. Recently, researchers investigating the possibility of using nanomaterials in welding processes at the nanoscale that a new chapter in the field of nanotechnology associated with welding is open.[3]

Fattahi *et al.*[4] have reported the improvement of impact toughness of the AWS E6010 weld metal, specifically when a medium TiO_2 nanoparticles content was added to the electrode coating. Also, Pal *et al.*[5] reported that the addition of nanoparticles of TiO_2 on coating of the coated AWS E11018M electrode was improved tensile and charpy impact property. Furthermore, Aghakhani *et al.*[6–9] have reported that the depth of penetration, heat affected zone width, and hardness of the melted zone were affected by the addition of TiO_2 and Cr_2O_3 nanoparticles to the weld pool.

Submerged arc welding (SAW) is an arc welding process widely applications in various industries due to its inherent advantages including ease of control of process parameters, depth of penetration, high metal deposition rate, smooth bead, ability to weld thick plates, and prevention of atmospheric contamination of the weld pool.[10,11] In this process similar to any other arc welding process, the high quality weld is mainly influenced by the independent input parameter including welding current, welding speed, arc voltage, and nozzle-to-plate distance since they are closely related to the geometry of weld bead, a relationship which is thought to be complicated because of the nonlinear characteristics. In order to attain the desired weld bead quality, the input parameters ought to be selected in appropriate combination and the correct choice of these parameters require adequate details about the effects of various input parameters on weld bead characteristic[12].

Response surface methodology (RSM) is commonly used in different fields such as chemistry, engineering, physics, and so on[13–16]. Box and Wilson developed central composite rotatable design (CCRD) as a design of RSM.[17] Box and Behnken offered another design of RSM.[18] A lot of attempts happen to be modeled the relationship between the important welding input parameters and weldment characteristics in SAW process.

Yang *et al.*[19] reported the application of linear regression model for computing the weld bead

MOHSEN KAZEMI, Master of Science Student, is with the Department of Mechanical Engineering, Islamic Azad University Science and Research of Kermanshah Branch, P. O. Box 67156 65195, Kermanshah, Iran. MASOOD AGHAKHANI, Assistant Professor, is with the Welding Research Center, Mechanical Engineering Department, Razi University, Kermanshah, Iran. EHSAN HAGHSHENAS-JAZI, Ph.D. Student, and ALI BEHMANESHFAR, Instructor at University, are with the Young Researchers and Elite Club, Najafabad Branch, Islamic Azad University, Najafabad, Isfahan, Iran. Contact e-mail: ali.behmaneshfar@gmail.com

Manuscript submitted on January 5, 2015.
Article published online November 6, 2015.

Table I. Input Parameters and Their Levels

	Notation	Coding					Units
Welding parameter		−2	−1	0	+1	+2	
Welding current	*A*	500	550	600	650	700	A
Arc voltage	*B*	24	26	28	30	32	V
Nozzle-to-plate distance	*C*	30	32.5	35	37.5	40	mm
Welding speed	*D*	300	350	400	450	500	mm/min
Thickness of MgO nanoparticles	*E*	0	0.25	0.5	0.75	1	mm

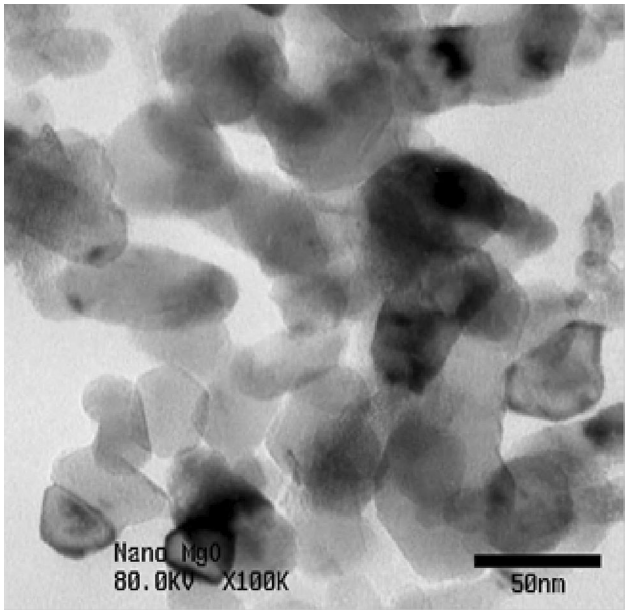

Fig. 1—TEM image of morphology MgO nanoparticles.[23]

geometrical features of the SAW process parameters. The results shown that the linear regression model was useful for computed the various geometrical features of the SAW process.

Murugan *et al.*[20–22] were developed mathematical models for SAW of pipes using RSM to predict and control of the weld bead parameters (penetration, reinforcement, width, and dilution) as affected by the welding input parameters (arc voltage, wire feed rate, welding speed, and nozzle-to-plate distance).

In the present work, first aim is to use RSM to relate the SAW welding input parameters current (*A*), arc voltage (*B*), nozzle-to-plate distance (*C*), welding speed (*D*), and MgO nanoparticles (*E*) to the prediction of the depth of penetration of St37 steel. The second aim is to find the optimal welding combination that would maximize the depth of penetration, keeping the cost relatively low.

II. MATERIALS AND METHODS

In the present paper, the effect of welding input parameters on the depth of penetration based on CCRD having five-level-five-factor each was examined. The welding current (*A*), arc voltage (*B*), welding speed (*D*), nozzle-to-plate distance (*C*), and thickness of MgO nanoparticles (*E*) were considered as the input parameters, respectively. These parameters and their levels are shown in Table I. The values of parameters were coded using the formula below.

$$x_i = \frac{X_i - \frac{(X_{\text{high}}+X_{\text{low}})}{2}}{\frac{X_{\text{high}}-X_{\text{low}}}{2}}, \quad [1]$$

where x_i is the coded value of *i*th factor, X_i is the real value (uncoded) of *i*th factor, and X_{high} and X_{low} are the high and low levels of *i*th factor in uncoded form, respectively.

The relationship between depended parameter (depth of penetration) and independent parameters (welding input parameters) were obtained using a quadratic polynomial model. This model is as follows:

$$Y = b_0 + \sum_{i=1}^{k} b_i x_i + \sum_{i=1}^{k-1} \sum_{j=2}^{k} b_{ij} x_i x_j + \sum_{i=1}^{k} b_{ii} x_i^2 + e, \quad [2]$$

where Y is the predicted response, b_0 is the constant term, b_i is the coefficient of the main effect of *i*th factor, b_{ij} is the coefficient of interaction effect between *i*th and *j*th factors, b_{ii} is the squared effect of *i*th factor, and e is the error.

The indices of quality of the model are R^2, R^2 (pred), R^2 (adj), and p value of regression. These indices are between zero and one. First to third indices should be big enough and p value closed to zero. Analysis of variance (ANOVA) is used to determine significant terms and p value of the model. All calculations were done using Minitab 16 software.

MgO nanoparticles supplied by Neutrino Co, Iran, were used as the input welding parameters. Figure 1 shows the TEM image of MgO nanoparticles. It can be seen that the morphologies of MgO nanoparticles are spherical. Also, the average particle size and specific surface are about 40 nm and 50 m^2/g, respectively. The characteristics of the nanoparticles are shown in Table II.

Prior to welding operation, workpiece dimensions of size 15 × 50 × 15mm^3 of St37 steel plates were cut and their surfaces were cleaned with acetone and coated with layers of MgO nanoparticles. Also, flux of agglomerated aluminate-rutile (AWS A5.17: F7AZ- EL12) type with the basicity index of 0.4 (Al_2O_3 + MnO55 pct, SiO_2 + TiO_2 30 pct and CaF_2 5 pct), copper-coated electrode wire with diameter of 3.2 mm in coil form with the type

Table II. Characteristic of MgO Nanoparticles[23]

Name	Appearance	Morphology	Specific Surface Area (m^2/g)	Average Particle Size (nm)	Purity (pct)
Magnesium oxide	white powder	spherical	>50	<40	99.9

Table III. Design of Matrix Based on CCRD

Standard Order	Run Order	*A*	*B*	*C*	*D*	*E*	Penetration (Actual)	Penetration (Predicted)
1	9	−1	−1	−1	−1	1	3.46	3.82632
2	21	1	−1	−1	−1	−1	2.4	2.32672
3	27	−1	1	−1	−1	−1	4.62	4.75508
4	10	1	1	−1	−1	1	3.03	3.43796
5	11	−1	−1	1	−1	−1	3.3	3.20088
6	22	1	−1	1	−1	1	3.13	3.16132
7	18	−1	1	1	−1	1	3.35	3.58964
8	5	1	1	1	−1	−1	5.8	5.74256
9	14	−1	−1	−1	1	−1	3.5	3.5492
10	25	1	−1	−1	1	1	2.07	2.35712
11	3	−1	1	−1	1	1	4.75	4.72048
12	7	1	1	−1	1	−1	5.85	5.72088
13	4	−1	−1	1	1	1	2.93	2.89632
14	15	1	−1	1	1	−1	2.54	2.54924
15	28	−1	1	1	1	−1	3.35	3.04256
16	20	1	1	1	1	1	3.09	2.87796
17	23	−2	0	0	0	0	3.91	3.77316
18	30	2	0	0	0	0	3.53	3.42148
19	32	0	−2	0	0	0	3.11	2.91446
20	6	0	2	0	0	0	5.37	5.41946
21	8	0	0	−2	0	0	4.59	4.05148
22	31	0	0	2	0	0	2.96	3.14316
23	2	0	0	0	−2	0	4.54	3.88816
24	29	0	0	0	2	0	3.3	3.30648
25	13	0	0	0	0	−2	3.27	3.57946
26	19	0	0	0	0	2	3.03	2.57446
27	1	0	0	0	0	0	3.63	3.59732
28	12	0	0	0	0	0	3.47	3.59732
29	16	0	0	0	0	0	3.3	3.59732
30	17	0	0	0	0	0	3.43	3.59732
31	24	0	0	0	0	0	3.52	3.59732
32	26	0	0	0	0	0	3.28	3.59732

of DIN S1 (AMA Co. Trade Name 50-11) and the angle of 90 deg between electrode and the workpiece were used in the process.

The experiments were performed by PARS CAT P2310 semi-automatic SAW equipment using direct current reverse polarity (DCRP) and the bead-on-plate weld was carried out in random order. In this research work, thirty two experiments were carried out as per the design matrix given in Table III. The specimens were cut perpendicular to welding direction and finishing with emery papers of grade 240, 320, 400, and 600 and etched with 2 pct Nital solution. Finally, the weld bead profile was measured by means of Olympus optical microscope and obtained the depth of penetration for each run are shown in Table III.

III. RESULTS AND DISCUSSION

The used design matrix is shown in Table III. In this matrix, standard order, run order, and levels of each factor are illustrated. ANOVA was carried out for the quadratic polynomial model. This model is used to determine five input parameters and called full model. The *p* value of each term is shown in Table IV. This model is as follows:

$$\begin{aligned}\text{Weld bead penetration} = {} & 3.487 - 0.0879A + 0.6263B \\ & - 0.2271C - 0.1454D - 0.2513E + 0.0216A^2 \\ & + 0.1516B^2 + 0.0353C^2 + 0.0716D^2 - 0.1209E^2 \\ & + 0.2969AB + 0.2881AC - 0.0381AD - 0.3119AE \\ & - 0.1956BC + 0.0931BD - 0.3281BE - 0.3956CD \\ & + 0.0356CE + 0.0469DE \end{aligned} \quad [3]$$

However, the *p* value of this model is great; some terms do not have acceptable *p* value. These terms are *A***A*, *C***C*, *D***D*, *A***D*, *B***D*, *C***E*, and *D***E*. Thus, ANOVA was done for the model without these terms, therefore this model is called reduced model. The *p* value of each term is illustrated in Table IV. This model is as follows:

$$\begin{aligned}\text{Weld bead penetration} &= 3.5973 - 0.0879A + 0.6263B - 0.2271C \\ &\quad - 0.1454D - 0.2513E + 0.1424B^2 - 0.1301E^2 \\ &\quad + 0.2969AB + 0.2881AC - 0.3119AE \\ &\quad - 0.1956BC - 0.3281BE - 0.3956CD\end{aligned} \quad [4]$$

Table IV. *p* Value of Each Term in Full Model

Source	*p* Value (Full Model)	*p* Value (Reduced Model)
Regression	0.001	0
Linear	0	0
A	0.283	0.213
B	0	0
C	0.014	0.004
D	0.089	0.047
E	0.008	0.002
Square	0.178	0.015
*A***A*	0.765	—
*B***B*	0.055	0.031
*C***C*	0.626	—
*D***D*	0.332	—
*E***E*	0.114	0.047
Interaction	0.002	0
*A***B*	0.01	0.002
*A***C*	0.012	0.003
*A***D*	0.697	—
*A***E*	0.008	0.001
*B***C*	0.065	0.031
*B***D*	0.35	—
*B***E*	0.006	0.001
*C***D*	0.002	0
*C***E*	0.716	—
*D***E*	0.633	—

In this model, the factors *A*, *B*, and *C* have main effect, but there are no quadratic terms of these factors. It means that variation of them affects the depth of penetration linearly. Since there are some interaction terms in this model, the level of factors should be considered in the existence of the other factors.

Adequacy of model was examined using analysis of residuals that includes normality assumption, independence assumption and constant variance assumption. Figure 2 shows normality assumption which is satisfied because all points are centered on straight line. Figure 3 shows the residuals *vs* the run order. Independence assumption is accepted by this figure because there isn't any trend among all points. Figure 4 exhibits residuals *vs* fitted values. There is no pattern in this plot, which is why constant variance assumption is satisfied.

Table 5 compares full and reduced models with regard to R^2, R^2 (pred), R^2 (adj), and *p* value. As can

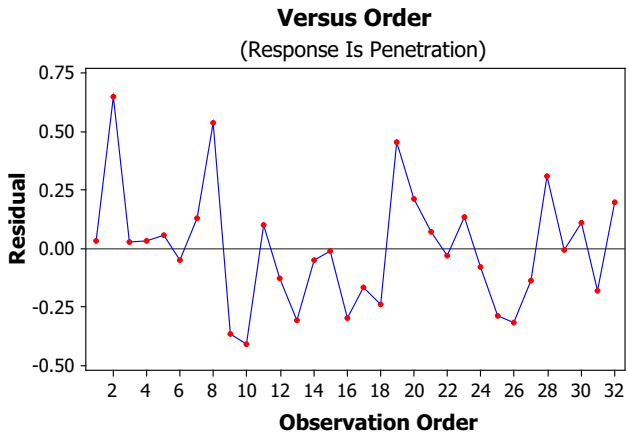

Fig. 3—Residuals *vs* the order of the data.

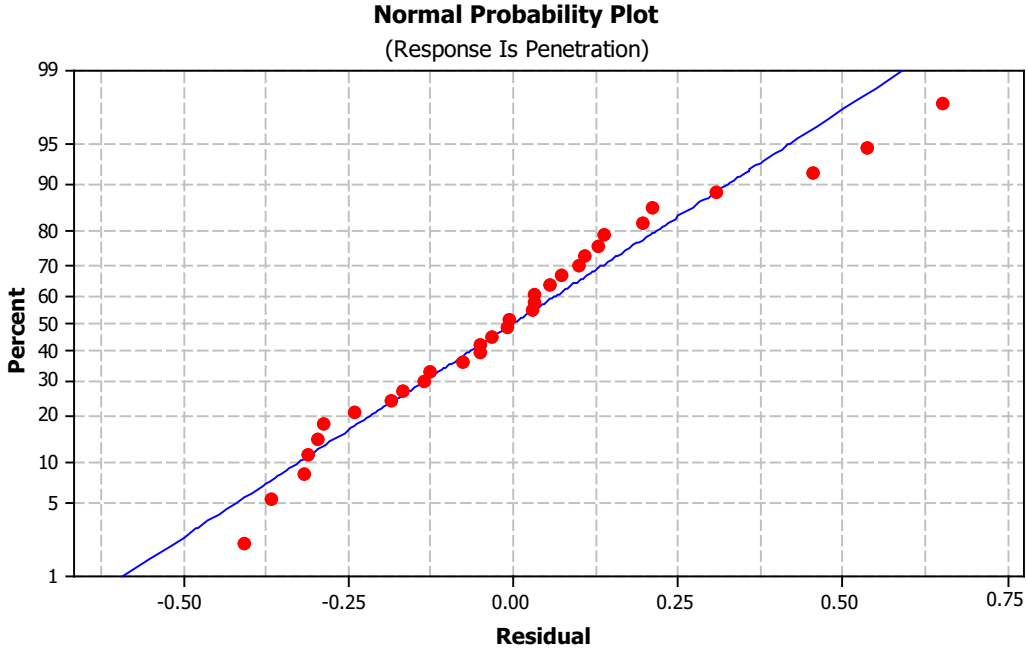

Fig. 2—Normal probability plot of the residuals.

Table V. Comparing Full and Reduced of Model

Model	R^2 (pct)	R^2 (pred) (pct)	R^2 (adj) (pct)	p value
Full model	93.63	0.00	82.06	0.001
Reduced model	92.05	69.05	86.31	0.000

Table VI. Optimum Levels of Factors

Name of Factor	A	B	C	D	E	Response
Value of factor	2	2	2	-2	−2	10.7624

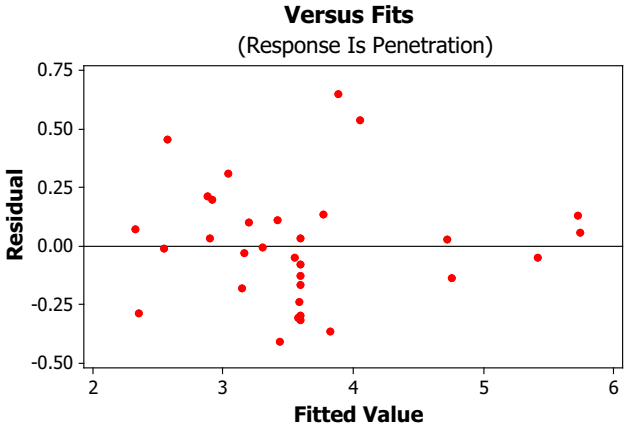

Fig. 4—Residuals *vs* the fitted value.

be seen, the reduced model is better than the full model based on mentioned criteria. R^2 (pred) value of full model is zero. However R^2 value of full model is better than reduced model, but there is no significant difference between R^2 values of these two models. Thus, the reduced model is used for predicting values of depth of penetration in different levels of factors. The values of predicted depth of penetration are shown in Table III.

The optimization of factor levels was carried out using reduced model and the results of optimization are shown in Table VI. Welding current, arc voltage and nozzle-to-plate distance should be adjusted in high level, whereas the welding speed and thickness of nanoparticles should be adjusted in low level. The value of depth of penetration is 10.7624 in this condition. The maximum value of the depth of penetration corresponds to the arc voltage of 32 V, welding current of 700 A, nozzle-to-plate distance of 40 mm, welding speed of 300 mm/min, and minimum thickness of the MgO nanoparticles is 0.0 mm.

The results can be used in companies which use submerged arc welding. Based on existing literature, it seems that researchers did not examine the effect of MgO nanoparticles as the additional flux on depth of penetration. The originality of this paper is to use MgO nanoparticles in submerged arc welding which provides suitable depth of penetration.

IV. CONCLUSIONS

From the results of the present research work, the following conclusions are summarized as follows:

- The five-level-five-factor CCRD techniques can be effectively used for predicting depth of penetration in the submerged arc welding within the range of parameters.
- The optimized quadratic polynomial model is shown that welding current, arc voltage, and nozzle-to-plate distance should be adjusted in high level, whereas the welding speed and thickness of nanoparticles should be adjusted in low level.

REFERENCES

1. J. Saurav: *Int. Eng. Res. App.*, 2012, vol. 2 (5), pp. 1077–82.
2. C. Suryanarayana and C.C. Koch: *Hyperfine Interact.*, 2000, vol. 130, pp. 5–44.
3. Y. Shangwei and H. Xuebao: *Trans. China Weld. Inst.*, 2007, vol. 28 (3), pp. 109–12.
4. M. Fattahi, N. Nabhani, M. Vaezi, and M. Rahimi: *Mater. Sci. Eng. A*, 2011, vol. 528, pp. 8031–39.
5. T.K. Pal and U.K. Maity: *Mater. Sci. Appl.*, 2011, vol. 2, pp. 1285–92.
6. M. Aghakhani, M.R. Ghaderi, A. Karami, and A.A. Derakhshan: *Int. Adv. Manuf. Technol.*, 2014, vol. 70 (1–4), pp. 63–72.
7. M. Aghakhani, M.R. Ghaderi, L. Rajabi, and A.A. Derakhshan: *Nanoeng. Nanomanuf.*, 2011, vol. 1, pp. 203–11.
8. M. Aghakhani, M.R. Ghaderi, A.H. Eslampanah, and S. Farzamnia: *Proceedings of 20th Annual International Conference on Mechanical Engineering, ISME*, April 2010, Shiraz, Iran, 2012.
9. M. Aghakhani and P. Naderian: *The 4th International Biennial Conference on Ultrafine Grained and Nanostructured Materials* (*UFGNSM*), Tehran, Iran, 5–6 November, 2013.
10. C.R. Heiple and P. Burgardt: *Metals Handbook Welding, Brazing, and Soldering*, American Society for Metals, Metals Park, Ohio, 1971, vol. 6, p. 67.
11. N. Murugan and V. Gunaraj: *Mater. Process. Technol.*, 2005, vol. 168, pp. 478–87.
12. P.T. Houldcroft: *Submerged Arc Welding*, 2nd ed., Woodhead Publishing Ltd, Cambridge, 1989, p. 67.
13. A.Z. Varzaneh, A.H.S. Kootenaei, J. Towfighi, and A. Mohamadalizadeh: *Anal. Appl. Pyrolysis*, 2013, vol. 102, pp. 144–153.
14. F. Gerayeli, F. Ghojavand, S.M. Mousavi, S. Yaghmaei, and F. Amiri: *Sep. Purif. Technol.*, 2013, vol. 118, pp. 151–61.
15. A. Hafizi, A. Ahmadpour, M.M. Heravi, F.F. Bamoharram, and M. Khosroshahi: *Chin. Catal.*, 2012, vol. 33 (3), pp. 494–501.

16. A. Behmaneshfar, M. Ghashang, M.R. Shafiee, A. Saffar-Teluri, A. Fazlinia, and H. Esfandiari: *Curr. Nanosci.*, 2015, vol. 11 (1), pp. 56–63.
17. G.E.P. Box and K. Wilson: *R. Stat. Soc.*, 1951, vol. 13, pp. 1–45.
18. G.E.P. Box and D.W. Behnken: *Technometrics*, 1960, vol. 2, pp. 455–75.
19. L.J. Yang, M.J. Bibby, and R.S. Chandel: *Mater. Process. Technol.*, 1993, vol. 39, pp. 33–42.
20. N. Murugan, R.S. Parmar, and S.K. Sud: *Mater. Process. Technol.*, 1993, vol. 37, pp. 767–80.
21. V. Gunaraj and N. Murugan: *Mater. Process. Technol.*, 1999, vol. 88, pp. 266–75.
22. N. Murugan and R.S. Parmar: *Mater. Process. Technol.*, 1994, vol. 41, pp. 381–98.
23. Neutrino Corporation. http://www.neunano.com/ [1August 2014].